Public document

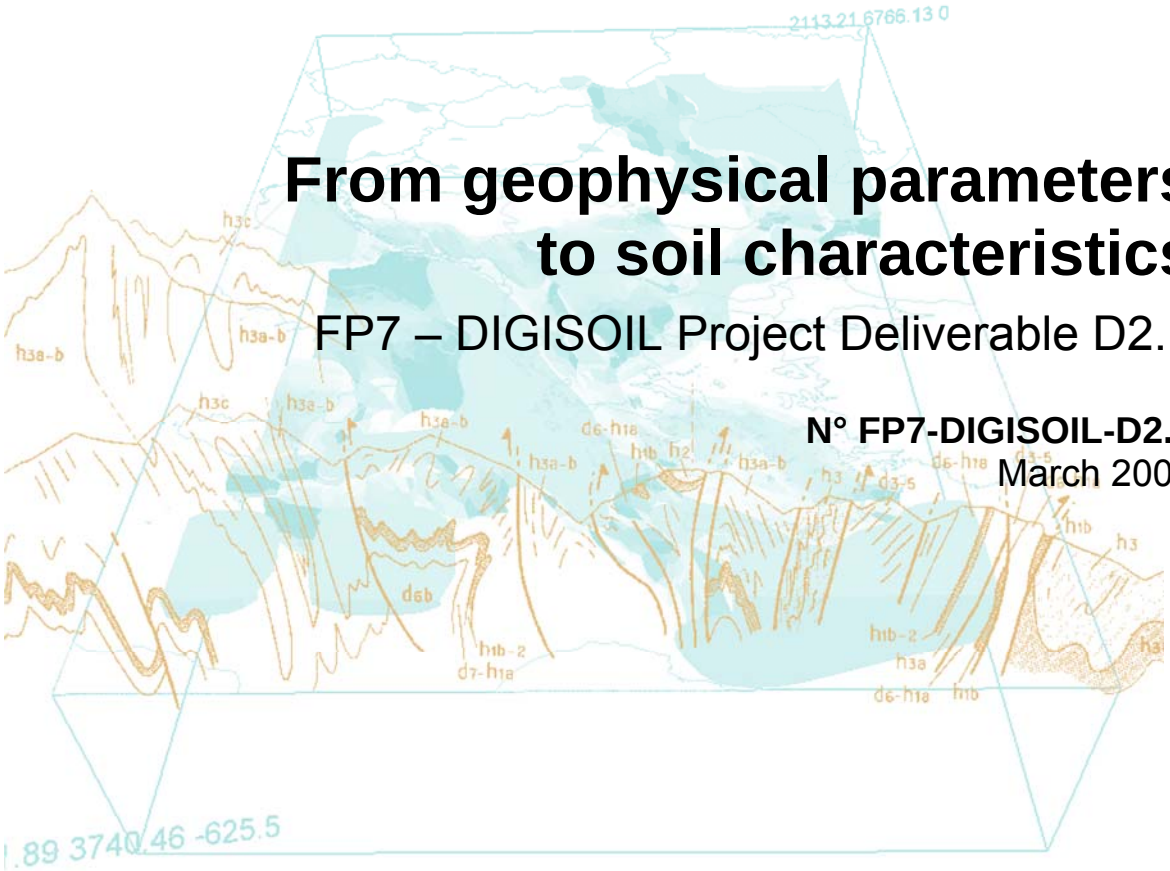

From geophysical parameters to soil characteristics

FP7 – DIGISOIL Project Deliverable D2.1

N° FP7-DIGISOIL-D2.1

March 2009

…

The DIGISOIL project (FP7-ENV-2007-1 N°211523) is financed by the European Commission under the 7th Framework Programme for Research and Technological Development, Area "Environment", Activity 6.3 "Environmental Technologies".

Geoscience for a sustainable Earth

brgm

Public document

From geophysical parameters to soil characteristics

FP7 – DIGISOIL Project Deliverable 2.1

FP7-DIGISOIL-D2.1
March 2009

G.Grandjean (BRGM)
With the collaboration of
I.Cousin, M.Seger, J.Thiesson (INRA), S.Lambot (UCL/FZJ), B.Van Wesemael, A.Stevens (UCL), K.Samyn, A.Bitri, S.Bernardie (BRGM)

Checked by:	**Approved by**:
Name: G.Grandjean	Name: I.Cousin
Date: 15/03/2009	Date: 20/03/2009
☑	☑

BRGM's quality management system is certified ISO 9001:2000 by AFAQ.

The DIGISOIL project (FP7-ENV-2007-1 N°211523) is financed by the European Commission under the 7th Framework Programme for Research and Technological Development, Area "Environment", Activity 6.3 "Environmental Technologies".

Geoscience for a sustainable Earth
brgm

Keywords: geophysical parameters, soil characteristics, data fusion.

In bibliography, this report should be cited as follows:
G.Grandjean, I.Cousin, M. Seger, J.Thiesson, S.Lambot, B.Van Wesemael, A.Stevens, K.Samyn, A.Bitri, S.Bernardie, 2009. From geophysical parameters to soil characteristics. Report N°BRGM/FP7-DIGISOIL-D2.1, 52 pages.

Synopsis

The purpose of this study concerns the review of all possible techniques for making the inversion of geophysical signals into physical parameters more robust. The information provided by the different sensors are thus be integrated in a complementary way using correction protocols and data fusion strategies. In that way, each sensor should contribute to constrain each other and regularize the overall integrated parameter estimations.

The present deliverable concerns the first task of the DIGISOIL's WP2. During this study, we analyze the requirements for making soil characteristic maps and the way to use and integrate geophysical parameters for this purpose. After a state of the art on the different solutions for assimilating different sources of information for improving the quality of such maps, we propose a review of the capabilities of each method for characterizing soil structures and soil properties.

A general processing workflow is established. It constitutes a first technical solution to reach our objectives. It will be tested in the future by using data acquired during the next field acquisition missions. This processing takes into account the different geophysical sensors already identified, supposes that inversion algorithms have already been applied to these data, uses auxiliary data for corrections, calibration or validation.

Contents

List of illustrations

1. Introduction

1.1. SUMMARY OF PROPOSED METHODS DELIVERING GEOPHYSICAL PARAMETERS

The purpose of this study concerns the review of all possible techniques for making the inversion of geophysical signals into physical parameters more robust. The information provided by the different sensors need first to be integrated in a complementary way using correction protocols and data fusion strategies. In that way, each sensor should contribute to constrain each other and regularize the overall integrated parameter estimations.

As specified in the project, and detailed in the D1.1, the following geophysical methods are considered in the DIGISOIL works:

Techniques (parameter)	Signal source	Sensors	Geometry	Piloting unit	Geolocalization	Limitations
Geoelectric (résisitivity)	DC	Electrodes	Quadripole Wienner	PC-based	Tracking GPS	High resistivity contrasts, buried pipes
EMI (conductivity)	VNA	VNA	Monostatic (array)	PC-based UCL/FZJ software	Tracking GPS piloted by the PC	EM noise
Magnetic (μ)	MVM, MS2, CS60, VC100	MVM, MS2, CS60, VC100	"Loop" (topsoil), Slingram (subsoil)	PC-based with INRA software	GPS	EM noise
GPR (dielectic constant)	VNA	VNA	Monostatic (array)	PC-based with UCL/FZJ software	Tracking GPS piloted by the PC	Too conductive shallow layers, strong soil roughness
Hyperspectral (reflectance)	Daylight	Optronics	Monostatic	GAV system	GPS	Vegetation, clouds, rain
Seismic (S-wave velocity)	Active source: 1 kg hand-driven hammer striking on a metal anvil	Geophones (10 Hz) plugged on a metal plate for moving	Linear seismic antenna composed by 24 geophones (10 Hz) and towed by a vehicle	PC-based system operating a GEODE acquisition unit with an adapted software (Geometrics)	Tracking GPS piloted by the PC.	Strong soil roughness

Table 1 : géophysical methods selected in the DIGISOIL project.

From the list of sensors and methods as depicted in Table 1, some redundancies between the delivered parameters can be observed, particularly for geoelectric, EMI and GPR, since these three sensors are sensitive to the soil electrical conductivity (inverse of the electrical resistivity). But these methods can also be complementary: GPR cannot generally sound the ground beyond the restricted domain of the top soil because of attenuation of the radar waves, while geoelectric is able to investigate deeper, depending on the electrode spacing. In addition to the listed methods, some corrections and calibration measurements have to be foreseen, either for improving the quality of the data or transform them into physical parameters more appropriate for the evaluation of the soil properties.

In order to take advantage of sensors and methods complementarities, an analysis of their contribution for mapping soil properties was carried out. This important step is presented in the next sections and constitutes the basis for designing the methodology for going from geophysical to soil properties maps.

1.2. GEOPHYSICAL METHODS VS SOIL CHARACTERISTICS DEPENDENCIES

In the context of the DIGISOIL project, five soil characteristics have been identified as parameters of interest, for developing indicators dealing with i) compaction, ii) decrease in organic matter, iii) erosion iv) shallow landslides.

These soil characteristics have already been identified as:

- bulk density
- texture (clay content)
- carbon content
- water content
- horizonation

From this list, three additional considerations need to be clarified before describing how they will be used in the next processing works.

The horizonation describes the fact that all the former parameters vary with depth along a soil profile. In soils, this variation with depth is usually a stepwise function because soils are most of the time recognised as composed of horizons, generally parallel to the surface. In the following, we will not consider the horizonation as a soil characteristic by itself. It will be taken into account by analysing the evolution of the soil properties with depth z, i.e., bulk density(z), texture(z), carbon content(z), water content(z), so that the characteristics of interest are restricted to four and vary along z.

The texture represents the granulometric composition of the soil, say the proportion of clay (particles<2µm), silt (2µm<particles<50µm), and sand (particles>50µm). The

carbon content is another variable of interest and will be considered separately. As far as mineral particles are concerned, the silt and sand fractions are usually constituted of feldspar and quartz particles, whereas the clay fraction is constituted of feldspar, quartz, iron-manganese oxides and mineral clay particles (smectites, illites, kaolinites, etc…). This clay fraction strongly modifies some geophysical parameters like the soil electrical conductivity or dielectric permittivity, for example. The clay content is therefore a more pertinent and quantitative characteristic than the “texture” and this soil characteristic will be analysed in the following.

Finally, at the season or annual scale, the clay content does not change in a given field area and, except when traffic or tillage operations are conducted in the field, the soil bulk density is supposed to be stable. The carbon content may significantly change after spreading of manure, but we will avoid such situations during our experiments. On the contrary, at these time scales, the soil water content varies significantly. Due to these variations, it becomes possible to characterise the soil hydraulic properties that are of interest to characterize most of the soil threats. As a consequence, we will characterise the water content as a function of time t.

These four soil characteristics are presented in the orange boxes in Figure 1. They can be determined from different physical parameters, as indicated by the colour arrows:

- Bulk density(z) can be determined from S-wave velocity, electrical conductivity and, to a lesser extent by magnetic susceptibility and viscosity.

- Clay content(z) can be determined from electrical conductivity, reflectance and, to a lesser extent by S-wave velocity.

- Carbon content(z) can be determined from magnetic susceptibility and viscosity, reflectance, and, to a lesser extent by electrical conductivity.

- Water content(z,t) can be determined from dielectric permittivity, and, to a lesser extent from electrical conductivity and reflectance.

Chapter 3 presents in detail the relationships between soil geophysical parameters and the four soil characteristics mentioned above.

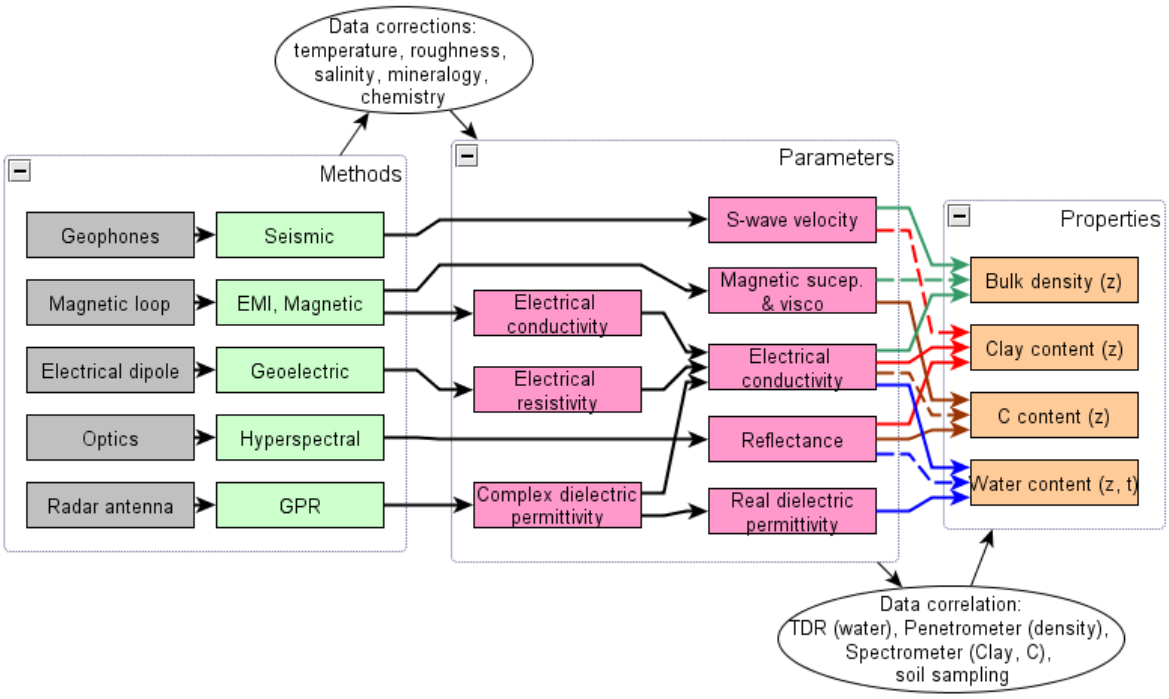

Figure 1 : diagram showing the different paths for going from sensors to soil properties.

1.3. PRINCIPLES OF DATA ASSIMILATION, CORRECTION AND CALIBRATION DATA

The transformation processes suggested by the Figure 1 are most of the time not straightforward and need to tackle some issues that will be discussed in the next chapters:

- Correction to be applied: some of the geophysical parameters, inverted from field measurements, are strongly dependent on time physical variables like temperature, water content, etc. When applicable, these corrections will be described and discussed in the framework of the next field measurement activities;

- Data calibration and assimilation: when transformations are more complex than simple physical or empirical relationships, more sophisticated methods, based on correlation or fusion strategies, can be used. These methods will be listed afterwards and described according to each of the geophysical parameters studied;

2. Techniques of combination and uncertainties management

2.1. GEOPHYSICAL DATA COMBINATION

Combining data is of an increasing interest since technological and industrial developments are able to provide complex systems of sensors for monitoring risky or protected areas from an environmental point of view. These sensor systems can either involve remote sensing or proximal airborne platforms, surface measuring geophysics or in-situ chemical/physical sensors. The way geophysical data can be combined into added-valued expressions depends essentially on two aspects:

- The level at which the combination is realized along the acquisition/processing flow: measuring the environment needs to activate a data acquisition flow going from the sensor to the information management board. Along this flow, signals are processed, improved and interpreted so that they become more specialized and dedicated to the finality. In principle, the more they propagate along the flow, the less they are generic;

- The knowledge of the measured object and its relationships with the considered geophysical parameters: this aspect decides how the processed data can be transformed into a soil characteristic qualifying the environment. This transformation can be direct if a direct and physical relationship exists between data and parameters; for the other cases, more indirect techniques have to be used.

These two aspects are developed in the following section.

2.1.1. Principle of data fusion in a multi-sensor approach

From sensors to soil characteristics

The typical processing flow going from the measured signals at a sensor to the interpreted soil characteristics characterizing the environment can be summarized as follow:

1. Analog signals are generated in the sensor as a response of some excitations produced in the observed environment;

2. Signals are digitalized in order to be transmitted easily, without quality decay, in the processing flow; eventually, signals coming from several sensors are combined and put in the same flow;

3. Digitalized Signals are interpreted in terms of geophysical parameters qualifying the observed environment, for example by data inversion processes;

4. Interpretation of the environment is performed by studying relationships between geophysical parameters and soils characteristics.

Because of a wide range of methods used in the Digisoil approach, combination of information can be foreseen at different levels. For example, inverted resistivity values obtained from geoelectric and EMI could be combined before their interpretation in terms of water content or clay content. The gain of such combination should be in the complementary capacities of these methods to measure resistivity with different resolutions, sensitivity or field conditions. For other methods, like seismic, the exploitation of the geophysical parameters (here Vs the S-wave velocity) will only be treated at the final level, during the inference process leading to the soil characteristics (here the soil bulk density).

Detailed processing flow concerning each of the proposed method will be presented afterwards, in section 3.

Methods for information fusion

2.1.2. The different techniques for combining informations

Estimating some quantities by the mean of information fusion, includes the combination of both data (as provided by the sensors) and process knowledge (expressed in terms of mathematical models). The information fusion strategy is closely related to the acquisition system, the level considered in the acquisition/processing flow and the relationship between the geophysical parameters and the soil characteristics, this last point being essential. We analyse in the next sections five common techniques of fusion depending on the complexity of this relationship.

Sensor level: data fusion using a Bayesian approach

At sensor level, two signals representing the same phenomenon and heaving the same mathematical features (format, sampling, numerical coding, etc) can be combined by using a Bayesian approach. Considering two events A and B, the Bayes theorem (Bayes, 1763) uses the probability theory for defining the *a posteriori* probability P(A/B) from two other sets: the likelihood function P(B/A) and the *a priori* probability P(A):

$$P(A/B) = \frac{P(B/A)P(A)}{P(B/A)P(A) + P(B/A^C)P(A^C)}$$

where superscript C is the complementary operator and P(A/B) means: “probability of A knowing B”. This expression is at the basis of the Kalman filter (Kalman, 1960) giving an explicit expression for combining two probabilistic values into a third one, taking into account their respective uncertainties. This filter can be efficiently used to merge two variables z_1 and z_2, using respective uncertainties σ_{z1} and σ_{z2}, into a more constrained variable $\hat{z}$.

$$\hat{z} = z_1 + K(z_2 - z_1), \quad \text{with } K = \frac{{\sigma_{z1}}^2}{{\sigma_{z1}}^2 + {\sigma_{z2}}^2} \quad \text{and } \frac{1}{\hat{\sigma}^2} = \frac{1}{{\sigma_{z1}}^2} + \frac{1}{{\sigma_{z2}}^2}$$

where K is known as the gain of the filter, and $\hat{\sigma}^2$ is the variance on the estimated variable $\hat{z}$.

Parameter level: physical laws

When trying to translate a geophysical parameter into a soil characteristic, the most direct solution, when possible, consists in using physical or empirical laws linking these two quantities.

For example, the Archie’s equation expresses the effective resistivity ρ_{eff} according to the water resistivity ρ_w and the formation factor F depending on the soil porosity (Thomas, 1992):

$$\rho_{eff} = F = \rho_w \frac{1}{\phi^m}$$

where m is a parameter that has to be fixed empirically and ϕ is the porosity.

Parameter level: data fusion using correlation techniques

When the translation from a geophysical parameter into a soil characteristic is not so straightforward, an alternative solution consists in studying the influence of the soil characteristic on the geophysical parameter, provided that studied data refer to the same field conditions.

As example, Schon (1996) shows a cross plot where the P-wave velocity varies according to the clay content for water-saturated marine sediments (Hamilton, 1970). This cross-plot is represented in Figure 2 and indicates that a relatively good dependence exists between these two quantities. Of course, using such a method needs to have access to a database sufficiently exhaustive for the correlation to be significant.

This strategy is also often used to retrieve soil properties from hyperspectral imagery. Since a given soil spectrum constitutes a mix of physical (texture, roughness, orientation) and chemical information, it is usually easier to quantify the property of interest using statistical techniques (*Chemometrics*) rather than physical laws.

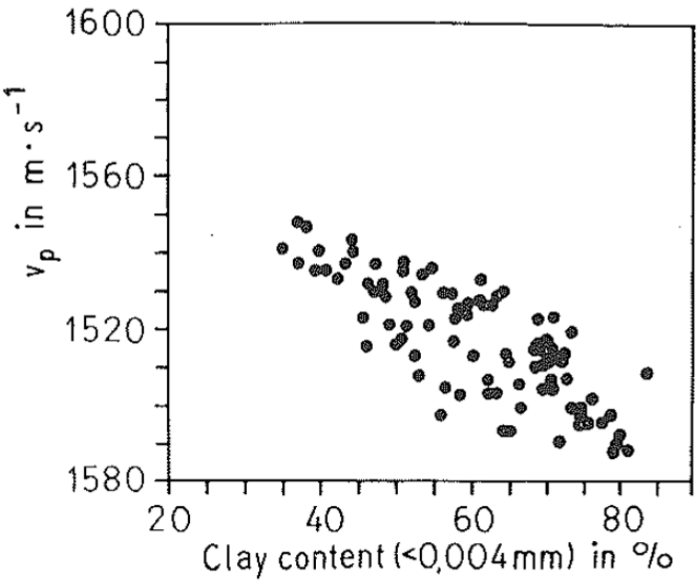

Figure 2 : Variation of Vp with clay content in water-saturated marine sediment (from Hamilton, 1970)

Parameter level: data fusion based on fuzzy logic

In some cases, physical or empirical relations do not exist or correlations are not sufficiently representative to be used as described above. These cases can nevertheless be considered if a thematic expert drives the transformation processes. Using this approach, the expert has to define some rules, known from its own experience that will be the basis of the translation of geophysical parameters into soil characteristics. Generally, and in the classical way of doing, the interpretation of geophysical data in terms of geological or pedological cross maps is carried out by this means.

Recently, for making such operations less subjective, new methodologies based on fuzzy logic have been tested to replace expert's interpretations. The principle consists in formulating the expert's rules into mathematical functions that are then used to transform geophysical data into soil interpretation (Figure 3).

Figure 4 shows an example where a 2D tomogram of the P-wave velocity (Vp) is combined with the likelihood function given by the inversion process to produce a possibility cross-section. This map indicates the place in the cross-section where it could be possible that the medium is fissured.

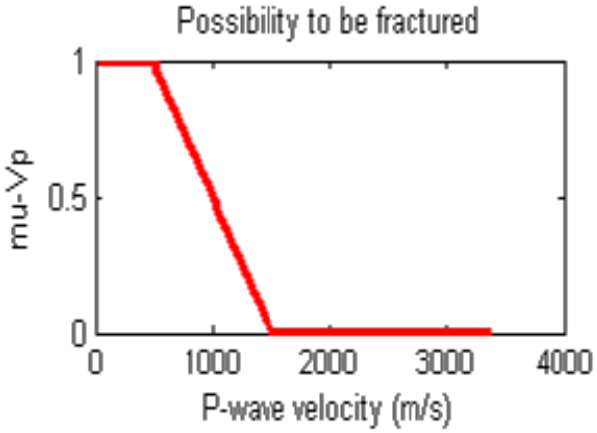

Figure 3 : belonging function used in fuzzy logic method. This function gives the possibility that a material is fissured depending on the value of Vp.

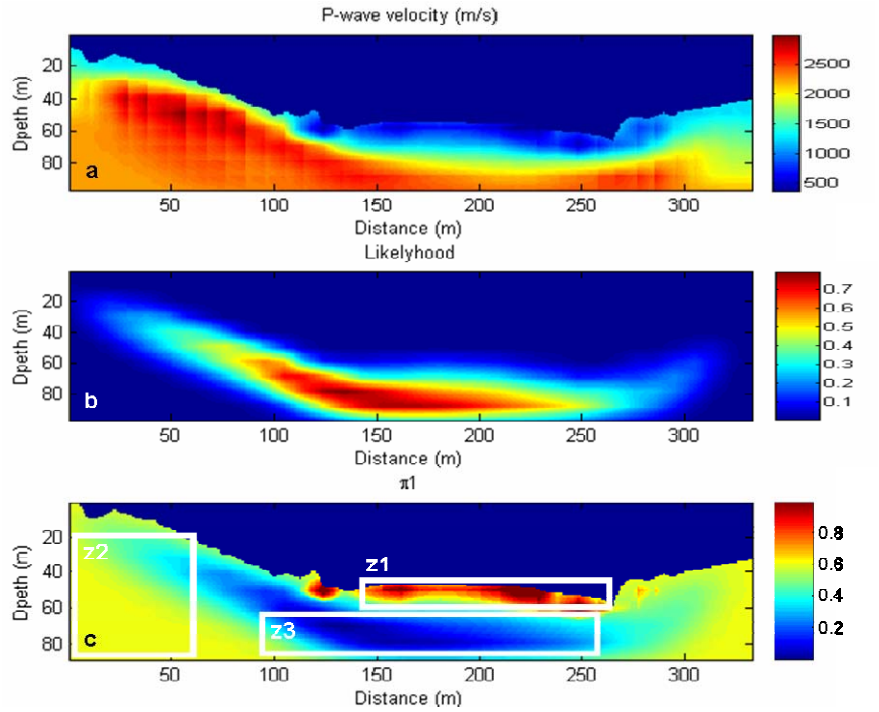

Figure 4 : Example of fuzzy logic rule for translating P-wave velocity (Vp) and its likelyhood function (LVp) into a map indicating the possibility (p1) that the rocks are fissured (Grandjean et al., 2007).

2.2. HOW TO MANAGE UNCERTAINTIES

Managing uncertainties may guaranty the quality of the soil properties maps that will be delivered to end-users. Each of the geophysical techniques, interpretations or fusion processes needs this aspect to be considered.

During the inverse modelling step that lead obtaining the geophysical parameters, the covariance matrix of the parameters can be estimated with linear regression analysis (approximated, but does not need large computing resources) or by Monte-Carlo-based simulations (large computation cost). The resulting uncertainty depends directly on the topography of the objective function (See D1.2).

Depending on the level the fusion and the kind of interpretation method, uncertainties will be defined and used as following:

- For fusion dealing with Kalman filtering, a variance value can be estimated since the *a priori* values are defined with their own variances;

- If empirical or physical relationships are used, an uncertainty function will be designed to compute the error propagated from the geophysical parameter to the soil property;

- In the case of correlation cross-plot, the dispersion of the scattered plot around the regression function will be used to recover the errors on estimated soil property values;

- For the fuzzy logic approach, Grandjean et al. (2007) demonstrated that it was possible to combine likelihood functions with the resulting parameters maps so that the possibility values in unconstrained areas of the studied domain can be identified.

3. Review of geophysical parameters and use of auxiliary data

Soil comes from a complex interaction between earth materials, climate, and organisms acting over time. Soil characterisation by sampling and in-situ testing (cone penetration, water content measurements, etc) faces unavoidable perturbation effects. On the other hand, geophysical techniques provide an effective alternative for site assessment. In particular, near surface site characterisation using seismic and electromagnetic methods yields important information related to the soil characteristics, including the spatial distribution of materials, small strain elastic properties and electromagnetic characteristics (Santamaria et al. 2005). In turn, geophysical measurements can be associated with soil parameters relevant to geotechnical or pedological engineering analysis. In the following sections, usefulness of such measurements for providing information on soil characteristics is discussed.

3.1. GEOELECTRIC

3.1.1. Data corrections

Introduction to the electrical resistivity in soils

Among the soil characteristics of interest in the DIGISOIL concept, the following have an influence on the soil electrical resistivity:

- the soil water content
- the soil texture (or soil clay content)
- the soil bulk density

Two other parameters influence also the soil electrical resistivity and will be discussed in the following:

- the soil temperature
- the chemical composition of the soil solution

In soils, the electrical resistivity depends to a large extent on electrolytes, say anions and cations. The free electrical charges that are responsible for the electrical resistivity are either carried by dissolved ions and participate to the volume conduction, or carried by the solid/liquid interfaces, and participate to the surface conduction. In soils, the volume conduction dominates, and, as a consequence, the electrical resistivity is very sensitive to the water content and, to a lesser extent, to the composition of the soil

solution. Let us now consider independently the influence of the different soil characteristics on the soil electrical resistivity.

Influence of the soil water content on the soil apparent electrical resistivity

Depending on the climate and on the cultural operations, and also on the soil water hydraulic conductivity, the water content varies strongly at a given location on the soil, and along the soil profile. As far as the soil electrical resistivity is concerned, one has to consider two cases: either the soil is saturated (i.e. all the porosity is filled by water), or the soil is unsaturated (i.e. the porosity is filled both by water and air). In the first case, the composition of the soil solution is important, whereas in the second case, it can be neglected under some assumptions (see later).

Lots of experimental works have demonstrated that the electrical resistivity increases when the water content decreases (Kalinski & Kelly, 1993; for example). Laboratory experiments showed that the relationship between the electrical resistivity and the water content is complex. The Archie's law presents the relationship between the electrical resistivity (or the electrical conductivity as presented here) and the water content:

$$\sigma / \sigma_w = \phi^m S^n$$

where σ represents the soil electrical conductivity, σ_w represents the water electrical conductivity, ϕ represents the soil porosity and S represents the degree of saturation. Parameter m is the coefficient of tortuosity and n is a fitting parameter.

Nevertheless, this law has been demonstrated in laboratory on model porous media and can not be directly applied for the soil, due to the number of parameters that influence the soil electrical resistivity. Moreover, in the range of variation of water content that is consistent for environmental and agronomic applications, a quasi-linear relationship between the soil water content and the soil electrical resistivity can be evidenced (Fukue et al., 1999).

Influence of the chemical composition of the soil solution on the soil apparent electrical resistivity

In soils, the electrical conduction is mainly related to the displacement of ions. As a consequence, the composition of the soil solution (i.e. the composition of the fluid inside the porous network of the soil) can influence the apparent electrical resistivity of the soil. Generally, the electrical resistivity data related to the soil solution are discussed in conductivity, the reverse of resistivity. The relationship between the soil apparent conductivity and the conductivity of the soil solution has been analysed for several decades on laboratory experiments (Shainberg et al., 1980; Rhoades et al. 1999; Hendrickx et al., 2002). It was demonstrated that, for a soil solution concentration higher than 40 mM, a linear relationship exists between the electrical conductivity of the soil solution and the apparent electrical conductivity of the soil. This threshold is quite high for soils and corresponds to salt soils or sodic soils. Under that threshold, this

relationship between the electrical conductivity of the soil solution and the apparent electrical conductivity of soil is not linear.

Influence of the soil texture on the soil apparent electrical resistivity

The nature of the soil particles that constitute the soil influences the electrical resistivity. As said before, the electrical resistivity in soil mainly depends on the displacement of ions. Nevertheless, in some conditions and especially when the soil contains clay, the surface conduction cannot be neglected and the apparent soil electrical resistivity is influenced by the clay content. The electrical resistivity of clay ranges from ~2 to ~100 ohm.m, whereas the electrical resistivity of sand is usually higher than 1000 ohm. (Samouëlian et al., 2005).

The organic matter content should also have an influence on the electrical resistivity but there is a lack of references on that subject in the literature.

Influence of the soil bulk density on the soil apparent electrical resistivity

The soil bulk density depends of the relative quantity of air and solid constituents in a given volume of soil. Let us consider a reference bulk density for a given soil; this bulk density can either decrease of increase.

Case 1: decrease of the bulk density. When the quantity of air in soil increases, say when the air-filled porosity increases, the electrical resistivity increases of several orders of magnitude. As a consequence, the electrical resistivity can be used to detect crack pattern in a soil when the latter dries. In that context, the electrical resistivity of the soil without crack is about 30-50 ohm.m, whereas the electrical resistivity of the cracked soil of the same texture can reach several hundreds of ohm.m. More generally, the electrical resistivity can be used to detect any increase of porosity due to cracking under drying, creation of tubular pores by the biological activity or creation of voids by ploughing or any tillage operations.

Case 2: increase of the soil bulk density. Under some cultural operations, the bulk density can increase, due to soil compaction. In that case, the electrical resistivity increases of several ohm.m. For example, for a loamy-clay soil at 0.3 m^3 m^{-3} water content, the electrical resistivity is of 40 ohm.m for a bulk density of 1.39 Mg m^{-3} and is of 30 ohm.m for the same soil after compaction (bulk density of 1.59 Mg m^{-3}) (Besson et al., 2004). Despite this small evolution of the electrical resistivity under bulk density, the latter can be discussed from electrical measurements when all the other parameters are under control.

Influence of the soil temperature on the soil apparent electrical resistivity

The temperature exhibits a strong variation along the soil profile: the first 20 cm are directly under the influence of climate and their temperature can vary of several degrees during one day, especially during summer under the sun. For the deeper layers, the temperature varies during the day but this variation is attenuated. Depending on the season, the top layers have a higher temperature (summer) or a

lower temperature (winter). Several models exist in the literature to take into account the variability of the soil temperature. Most of them are based on experiments on soil solutions: Campbell et al. (1948), Keller & Frischknecht (1966), for example. A recent review of all the models that are available to take into account the effect of temperature in measurements of soil electrical resistivity is given in Besson et al. (2008). It is recognised that the variation of the soil electrical resistivity is of 2 % per degree Celsius. In the top layers of soils, where the temperature can vary of several degrees per day, and where the order of the soil electrical resistivity is 25-80 ohm.m, the effect of the temperature can not be neglected in the interpretation of the measurements. We therefore recommend that a measurement of the soil temperature is associated to each electrical resistivity campaign, so that the corrections can be done. PT100 probes can be installed in the soil at different levels to record the soil temperature.

3.1.2. Contribution to soil properties mapping

Hierarchy between the different soil characteristics that influence the electrical resistivity

As a porous medium, the soil is composed of three phases: solid constituents - that can be clay, quartz, organic matter, etc -, water and air. The resistivity of air is that large that the influence of porosity dominates when the soil is really dry, say during summer. As a consequence, we can define roughly two periods during which the electrical resistivity is efficient or not to characterise a soil characteristic of interest in the DIGISOIL project.

Case 1: during summer, under very dry conditions.

In this context, the effect of porosity dominates and this period is favourable to characterise the soil bulk density, especially in a very porous soil. When the porosity is not that high, we can use the electrical resistivity to discriminate soils with different textures.

Case 2: during winter, under wet conditions.

In that context, the porosity is filled or almost filled with water and the resistivity is highly sensitive to soil water. On a small area, it can be difficult to identify soils with different textures because the water quantity hides differences due to textures. The determination of compacted or non compacted zones can usually not be determined during this period.

To use the electrical resistivity to characterise the water content, we suggest realising electrical resistivity measurements at different dates during one season. At this time scale, the other soil characteristics that influence the electrical resistivity do not change and the evolution of the electrical resistivity are only due to differences in water content (Besson et al., 2009). A simple relationship established from empirical observations can be used to transform the resistivity differences into water content variations as suggested by Figure 5. In dry conditions, correlations between observations of soil textures and resistivity variations can provide information on clay content.

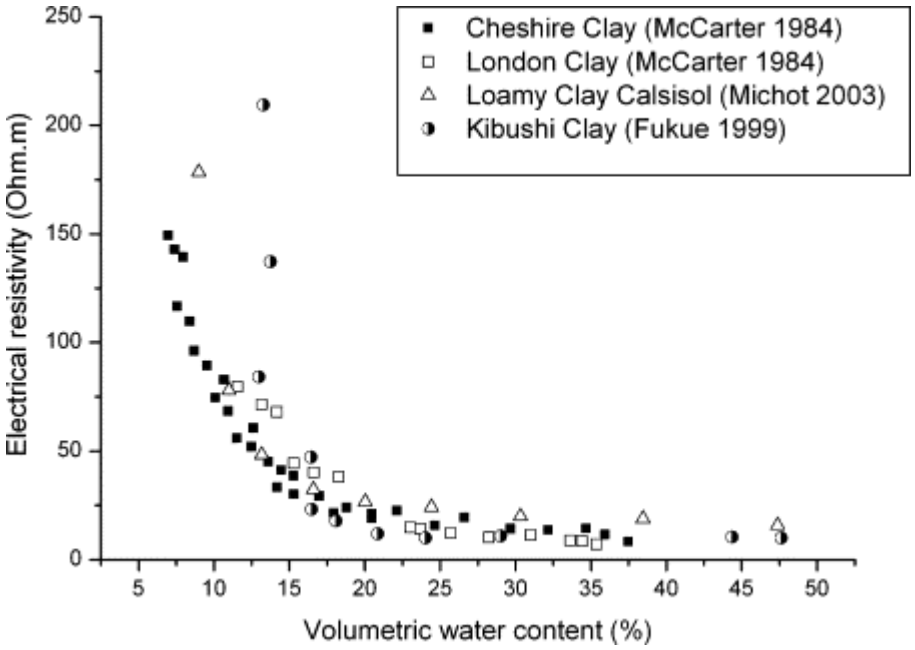

Figure 5 : Relationship between the volumetric water content and the electrical resistivity for different soil types (values issues from Fukue et al., 1999, Michot et al., 2003 and McCarter, 1984).

Finally, the difficulties occur when the soil bulk density evolves rapidly under the effect of modifications of water content, among others[1]. For example, a compacted zone can be created by traffic in wet conditions, usually in autumn. This compacted zone can be cracked under the effect of climate during the spring, when the water content of the soil decreases by evaporation. In that case, the evolution of the electrical resistivity depends on the decrease of water content and the increase of bulk density. The relative contribution of these two soil characteristics can be difficult to determine. This is a key-point in the interpretation of electrical resistivity in terms of mapping of soil characteristics.

How to take into account the effect of temperature and of the composition of the soil solution?

As said before, the electrical resistivity depends on some soil characteristics that are not of interest in the DIGISOIL program, especially the composition of the soil solution and the temperature.

[1] Let us note that the bulk density can evolve also either under the effect of frost/thaw or due to perforation by worms or roots, or by tillage operations.

As far as the temperature is concerned, the effect of this soil characteristic is of first-order and can not be neglected, especially in the case of the interpretation of measurements at several dates in the year on one site. We therefore advice to measure independently the soil temperature, for example by using PT100 probes. Electrical resistivity data could then be recalculated at a reference temperature by a correction equation. The correction equation usually used in the literature is the Keller & Frischknecht equation (1966), and the reference temperature is usually equal to 25°C.

As far as the composition of the soil solution is concerned, we can consider that this characteristic is of second-order for the soils of the validation sites and test sites in the DIGISOIL project. Indeed, these soils are neither sodic nor salt soils and, if we do not run experiments immediately after the fertilization periods, the composition of the soil solution could be neglected.

Quality of the estimation of soil characteristics in relation to depth

Electrical resistivity measurements from the soil surface are apparent measurements. To obtain an estimation of a soil characteristic, whatever it is, these apparent measurements can be discussed in that state or can be interpreted through an inversion model – like the Res2DInv program of Loke & Barker (1999) for example - to provide interpreted resistivity measurements. In case of using a model, the quality of the interpreted resistivity values depends on depth: the accuracy of the interpreted resistivity values decreases with depth. As a consequence, the quality of the interpretation of one soil characteristic with depth decreases.

3.2. EMI

3.2.1. Data corrections

Electrical conductivity (usually referred to as *EC* or σ) is the key soil geophysical parameter that is determined by electromagnetic induction (EMI). By definition, it is the inverse of electrical resistivity (ρ). As a result, the soil characteristics to take into account for the analysis and the interpretation of EMI-derived electrical conductivity data are identical to those mentioned in the context of geoelectrical methods (see Section 3.1) as influencing soil electrical resistivity. Given the equivalence between soil electrical conductivity and resistivity, we cover in this section only the concepts that are more specific to EMI research. We refer to Section 3.1. for further details. We have to stress that we consider here the “quasi-static” electrical conductivity, i.e., measured in the frequency range from 100 Hz to several kHz; at lower frequencies the electrodes polarisation interferes with the readings, while at higher frequencies (typically > MHz) the electrical conductivity is no longer constant as it increases with frequency as a result of dispersion phenomenon. In that later case, we refer to an “apparent” electrical conductivity, including dielectric losses.

Soil electrical conductivity results from the contributions of three pathways of current flow through the soil: (1) a solid-liquid phase pathway occurring mainly via

exchangeable cations associated with clay minerals, (2) a liquid phase pathway via dissolved solids contained in the soil water located in the large pores and (3) a solid pathway via soil particles in direct and continuous contact with one another (Figure 6). Rhoades *et al*. (1976) presented a simple linear model relating soil electrical conductivity to liquid-phase electrical conductivity, to water content and to dry soil electrical conductivity:

$$\sigma = \left(a\theta^2 + b\theta\right)\sigma_w + \sigma_s$$

where σ is the bulk soil electrical conductivity (S.m^{-1}), θ is the volumetric soil water content (m³.m^{-3}), σ_w is the soil solution electrical conductivity (S.m^{-1}), σ_s is the electrical conductivity of dry soil (S.m^{-1}), and *a* and *b* are soil specific empirical parameters. Later, Rhoades et al. (1989) developed a more sophisticated electrical conductance model considering more explicitly the three aforementioned current flow pathways, allowing to estimate soil electrical conductivity and to investigate its sensitivity to variations of soil properties; Lesch and Corwin (2003) extended the applicability of this model to extremely dry soil conditions.

The contribution of each pathway to the bulk electrical conductivity depends on several factors, which may we grouped into three categories: (i) factors referring to the *bulk soil* which define the respective volumetric fractions occupied by the three solid-liquid-air phases and their possible structural configurations (i.e., porosity, water content and structure), (ii) *solid particle* quantifiers (i.e., particle shape and orientation, particle-size distribution, cation exchange capacity and wettability), and (iii), *soil solution* attributes (i.e., ionic strength, cation composition and temperature). Amongst these factors, **water content** and the **composition of the soil solution** are generally the dominating soil characteristics in determining soil electrical conductivity; their influence may be investigated on the basis of the Archie's empirical law, which considers also the geometry and the topology of the aqueous phase (see 3.1). Nevertheless, except for coarse-textured soils or in case of very high ionic strength of the soil solution, the contribution to electrical conductivity of the ions adsorbed on **clay** particles cannot be neglected; it is determined mostly by the cation exchange capacity of the soil. Furthermore, variations of the soil **bulk density**, accompanied with changes in the 3-D configuration and/or in the relative importance of the solid-liquid-air phases, may also affect soil electrical conductivity (see 3.1). Finally, electrolytic conductivity increases at a rate of approximately 1.9% per °C increase in **temperature**. For the sake of comparison, electrical conductivity is usually expressed at a reference temperature of 25°C, and measurements at other temperatures have to be adjusted to this reference temperature using a conversion factor (Sheets and Hendrickx, 1995; Wraith and Or, 1999); this is particularly important for the upper soil layer more subject to rather large variations of temperature. In other respects, correction of electrical conductivity data is also sometimes requested to account for the variations of the sensor temperature during the measurement campaign (Robinson et al., 2004). As a reminder, water content, clay content and bulk density are of particular interest in the framework of the DIGISOIL project.

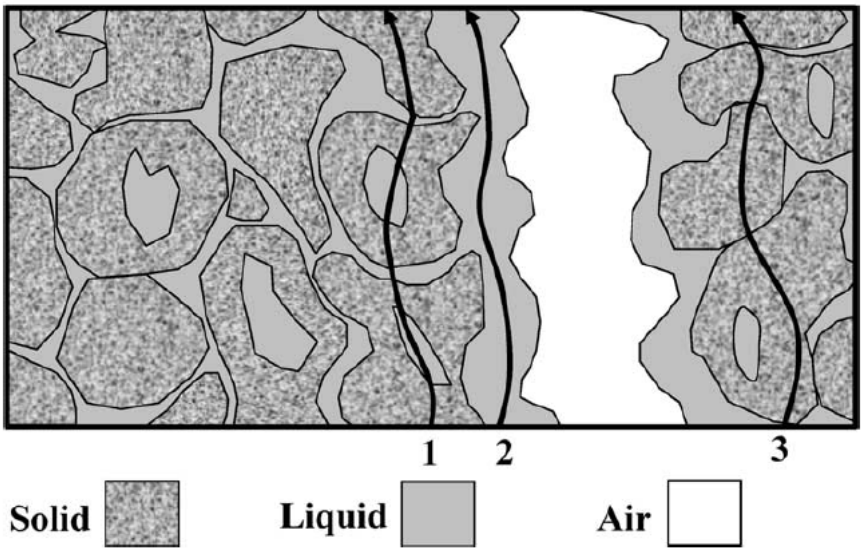

Figure 6 : Pathways of electrical conductance in soils (Corwin and Lesch, 2005).

3.2.2. Contribution to soil properties mapping

As stated above, soil electrical conductivity integrates several factors, which complicates the analysis of its spatial and temporal variations if more than one influencing soil characteristic varies at the same time. Nevertheless, interpretation of electrical conductivity data may be strongly alleviated by repeating measurements at different dates on a same site, as well as by combining EMI data with other sources of information.

As aforementioned for the interpretation of electrical resistivity data, performing time-lapse EMI measurements for different soil moisture conditions would allow for a more detailed characterisation of the soil properties, as a result of the contrasted electrical conductivities of the solid-liquid-gas phases (see above). Indeed, under wet conditions, electrical conductivity measurements are dominated by the effect of water content, which tends to hide the influence of the other factors. In contrast, dry conditions are much more favourable for the characterisation of soil bulk density or, for soils with intermediate or low porosity, of soil texture. Therefore, EMI data collected at different dates during one season would allow retrieving the variation of soil water content, assuming that the other soil characteristics are stable at this time scale.

Besides, joint inversion of EMI data with data from other geophysical sensors would also significantly improve the estimation of the soil properties, thereby unravelling the different contributions to a single measurement. For instance, the high sensitivity of GPR data to soil water content could be used to subtract the influence of this variable from simultaneously collected EMI data in order to assess other soil property(ies) with a greater accuracy, such as the electrical conductivity of the soil solution (salinity). Furthermore, integration of additional sources of information, not only in terms of data but also in terms of concepts, such as hydrodynamic laws or petrophysical

relationships, could also help to better constrain the overall estimation problem (Jadoon et al., 2008; Lambot et al., 2006).

The effect of temperature on soil electrical conductivity measurements may be taken into account by simultaneously recording the soil and, if necessary, the instrument temperatures and by applying the requested corrections. Soil temperature profiles may be estimated by applying a temperature transfer model subject to the climatic conditions as a first approximation. This temperature can be further constrained based on infrared images of the soil surface for surface temperature, and when possible, by inserting temperature sensors at several depths at key locations in the fields.

Vertical electrical conductivity profiles and corresponding variations of soil characteristics with depth could potentially be retrieved by performing measurements at several frequencies and/or with different sensor configurations (i.e., horizontal and vertical dipoles for different sensitivities with respect to depth) and by inverting these data using a modelling approach considering wave propagation in a multilayered medium, such as the method developed by Lambot et al. (2004a,b).

3.3. MAGNETISM

3.3.1. Data corrections

Two kinds of corrections on magnetism data are identified: measurement surface artefacts and acquisition systems thermal drift.

While the parameters influencing the magnetic signal of soils are the soil iron oxides grains, some disturbing iron artefacts may exist at field surface. Corresponding erroneous values (outliers) must be eliminated by filtering (for example median filtering on a moving window).

Some of the acquisition devices could present a thermal drift that can be corrected by using two approaches:

- A zero value is done in the air (free space measurement) far from any magnetic object between each measurement point.

- The drift is evaluated with a measurement at a given location called base with a regular time step (e.g. between each profile). Then this drift is interpolated and is subtracted to the measured signal at each point.

3.3.2. Contribution to soil properties mapping

The magnetic properties of soils, magnetic susceptibility (κ_{ph}) and magnetic viscosity (κ_{qu}) are linked to the amount of iron oxides in the soils and to the sizes of iron oxides grains. As these iron oxides, particularly viscous ones, partly originate from bacterial activities, it exists a link between organic matter content and magnetic properties.

The magnetic properties mapping would be used as a proxy for organic matter content mapping. Since the correlation between magnetic properties and organic matter content is established but not theoretically demonstrated, this relationship has for the instance to be determined using soil sampling and laboratory measurements.

3.4. GPR

3.4.1. Data corrections

GPR wave propagation in the soil is governed by the soil electromagnetic properties, namely, the frequency-dependent soil dielectric permittivity ε (determining wave velocity), electrical conductivity σ (determining wave attenuation), magnetic permeability μ (determining wave velocity, affects attenuation), and their spatial distribution. Provided sufficient sensitivity of the radar measurements to these parameters, these can potentially be retrieved from the GPR data using inversion techniques. For non-magnetic materials as prevalent in the environment, μ is equal to the free-space magnetic permeability μ_0; this parameter is therefore usually disregarded in GPR signal processing. The relative dielectric permittivity, or also referred to as dielectric constant κ, is defined as $\varepsilon_r = \varepsilon / \varepsilon_0$, where ε_r is the free space dielectric permittivity.

Due to the overwhelming dielectric permittivity of water compared to other soil constituents, the soil dielectric permittivity is highly correlated to its volumetric water content (Hilhorst, 1998; Topp et al., 1980). The relative dielectric permittivity of air is 1, of water is 80, and of dry natural geologic materials (with air in pore spaces) is approximately 3-8 ; hence, addition of water to the soil pore space drastically increases the dielectric permittivity of the soil. Other factors affecting the soil dielectric permittivity are the soil texture, organic matter content, porosity, and temperature. Yet, to some extent, the effect of these factors is secondary compared to the effect of water and these parameters are usually neglected. Several models are available to relate soil dielectric permittivity to volumetric soil water content (θ). The most used in soil physics is the empirical Topp's model :

$$\theta = -5.3\times10^{-2} + 2.92\times10^{-2}\varepsilon_r - 5.5\times10^{-4}\varepsilon_r^2 + 4.3\times10^{-6}\varepsilon_r^3$$

which was determined for mineral soils having various textures. It has an accuracy of 0.022 determined in an independent validation on mineral soils (Jacobsen and Schjonning, 1994). A more theoretical approach to relating soil water content and dielectric permittivity is based on dielectric mixing models, which use the volume fractions and the dielectric permittivity of each soil constituent to derive a relationship (Dobson et al., 1985). In dielectric mixing models, the bulk permittivity of a soil-water-air system may be expressed with the Complex Refractive Index Model (CRIM):

$$\varepsilon_r = \left(\theta\varepsilon_{r,w}^{\alpha} + (1-n)\varepsilon_{r,s}^{\alpha} + (n-\theta)\varepsilon_{r,a}^{\alpha}\right)^{\frac{1}{\alpha}}$$

where *n* is the soil porosity, $\varepsilon_{r,w}, \varepsilon_{r,s}, \text{and } \varepsilon_{r,a}$ are the permittivities of water, soil particles, and air, respectively; and α is a factor accounting for the orientation of the electrical field with respect to the geometry of the medium ($\alpha = 0.5$ for an isotropic medium). After substitution of $\varepsilon_{r,a}$ by 1 and α by 0.5, this model reduces to:

$$\theta = \frac{1}{\sqrt{\varepsilon_{r,w}} - 1}\sqrt{\varepsilon_r} - \frac{(1-n)\sqrt{\varepsilon_s} - n}{\sqrt{\varepsilon_w} - 1}\left(\theta\varepsilon_{r,w}^{\alpha} + \varepsilon_{r,s}^{\alpha} + (n-\theta)\varepsilon_{r,a}^{\alpha}\right)^{\frac{1}{\alpha}}$$

which gives a physical interpretation of a simple soil water content – dielectric permittivity relationship proposed by (Ledieu et al., 1986), namely:

$$\theta = a\sqrt{\varepsilon_r} - b$$

where *a* and *b* are calibration parameters depending on the soil type. For more information, the reader is referred to (Robinson et al., 2003).

It is worth noting that most available calibrations for these equations were derived using time domain reflectometry (TDR), which mainly operates in the frequency range 50-1000 MHz. However, it has long been recognized that high clay contents lead to significant permittivity dispersion in that frequency range (Lambot et al., 2005; West et al., 2003). Hence, depending on the operating frequency range used for GPR for a specific application and soil type, specific calibrations may be required for improved accuracy in soil water content estimation (Huisman et al., 2001; Lambot et al., 2004; Weiler et al., 1998).

In addition to dielectric permittivity, soil electrical conductivity can also be retrieved from the GPR data. The relationship between this variable and the soil properties has already been discussed in Sections 3.1 and 3.2. As emphasized above, in the GPR frequency ranges (UHF-VHF), dielectric losses become significant. Hence, the GPR-derived electrical conductivity simultaneously includes both conduction and relaxation effects (apparent electrical conductivity). In that respect, the electrical conductivity measured by a GPR is expected to be different (higher) compared to estimations from geoelectric and EMI methods, depending on the soil type. (Lambot et al., 2004; Lambot et al., 2005) showed that above 1 GHz, free water relaxation effects for a sandy soil are significant, while the dielectric permittivity remained constant at least up to 3 GHz.

3.4.2. Contribution to soil properties mapping

Mapping the soil dielectric permittivity permits to infer a series of important soil properties in addition to volumetric water content. When the soil is saturated, the water content directly provides a measure of the soil porosity. When the soil is completely dry, the dielectric permittivity depends mainly on the porosity and soil mineralogy, thereby providing information on these quantities. Performing time-lapse measurements during hydrodynamic events further permits to monitor these events, and by applying integrated inversion procedures, provides an estimation of the soil

hydraulic properties governing water flow in the soil (Jadoon et al., 2008; Kowalsky et al., 2005; Lambot et al., 2006). The vertical distribution of the soil dielectric permittivity also permits to identify subsurface structures such as layering (e.g., the bedrock). It is worth noting that each frequency component in the GPR data constitutes a piece of information, and therefore, wider is the frequency range, wider is the information content in the data. Yet, reconstruction of the soil dielectric permittivity with respect to depth is not an easy task and constitutes inherently an ill-posed inverse problem. That is why combining GPR information with data from other sensors and process knowledge using models is necessary. In particular, estimating the soil electrical conductivity at the geoelectric, EMI, and GPR frequencies will provide valuable information regarding the frequency dependence of the apparent electrical conductivity, and hence, provide information on the soil textural composition and structure. The redundant information between the sensors is further necessary to reduce uncertainty in the estimations.

3.5. HYPERSPECTRAL

3.5.1. Data corrections

In principle, any object reflects the same proportion of light independently of the light source or its environment. Unfortunately, some factors like atmosphere absorption and scattering, surface scattering, illumination geometry and shadowing influence and disturb the measurements of reflectance. Moreover, all things being equal, each sensor will produce different spectra for the same object due to internal characteristics of the instrument (*e.g.* spectral sampling interval, spectral calibration).

The radiometric calibration (sensor failure and calibration) is usually done by the manufacturer itself. At-sensor radiance is further corrected for atmospheric attenuations (Rayleigh/Mie scattering and absorption by water vapour, carbon dioxide and ozone), variation in source illumination (incoming solar energy) and geometry, as well as adjacency effects. There are several techniques available to correct for these phenomena. These can be classified in (i) scene-derived corrections (e.g. flat field correction), (ii) ground-calibrating methods (e.g. empirical-line calibration), and (iii) radiative transfer models (e.g. MODerate spectral resolution atmospheric TRANsmittance algorithm and computer model – MODTRAN from the Air Force Research Lab, Space Vehicles Directorate, USA). The latter codes are used to predict atmospheric radiative properties and model at-sensor radiance. They are generally embedded in atmospheric correction models (e.g. ATCOR, FLAASH, HATCH) which require measured or modelled input variables such as atmospheric conditions (optical depth,…) and geometry information (flight altitude, illumination and viewing angles,…). Geometric correction may be accomplished before or after atmospheric correction. Geometric distortions may be caused by the geometric characteristics of the sensor itself, variation in the position and orientation of the sensor (pitch, yaw and roll) and relief displacement. Ortho-rectification can be realized (i) with Ground Control Points (GCPs) and polynomial functions or (ii) with model-based corrections (direct georefencing, see e.g. PARGE, ReSe Applications Schäpfler & RSL, University of Zurich). The latter method exploits Inertial Navigation System (INS) and differentially-

corrected GPS data (lat, long, height) recorded in the aircraft to ortho-rectify an image over a Digital Elevation Model (DEM).

There is an anisotropy in the directional distribution of the solar radiation scattered from the surface which results in a variability in the measured at-sensor radiance as a function of viewing/illumination geometry and micro-topography. These effects, known as Bidirectional Reflectance Distribution Function (BRDF), are usually taken into account in a very crude way within atmospheric correction algorithms. This phenomenon is illustrated in Figure 7 showing soil reflectance pixels from an airborne hyperspectral sensor (AHS-160) at selected wavelengths as a function of view zenith angle. From a maximum reflectance peak located near -40° of view zenith angle (backscattering position), reflectance decreases progressively towards the nadir and forward scattering position (+40°). Such figures are typical of rough surfaces. The main explanation can be found in the change in the proportion of illuminated *vs* shadowed areas as a function of viewing geometry (see e.g. Cierniewski and Courault, 1993). The methodology proposed by Feingersh, et al. (2009), involving laboratory measurements and image processing, can be implemented to remove such effect.

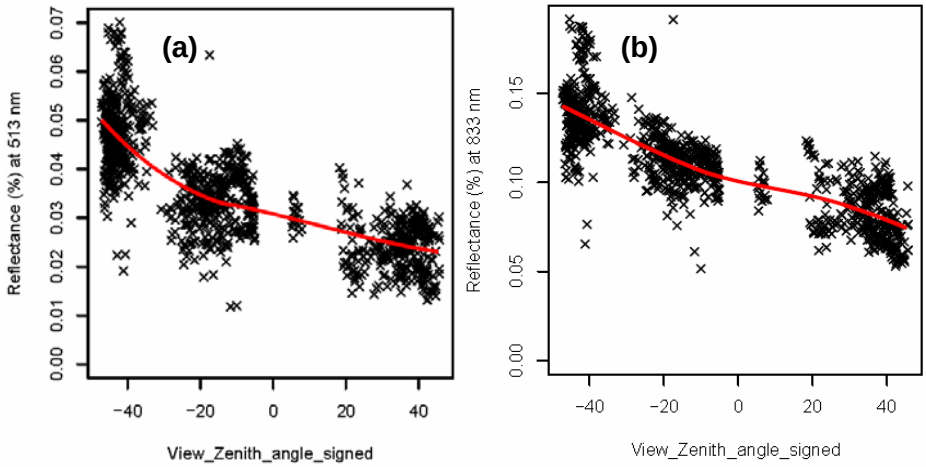

Figure 7: Reflectance of soil pixels at (a) 513 nm and (b) 833 nm as a function of viewing angle.

After geometric and atmospheric corrections, several mathematical pre-treatments are still necessary. Basically, these operations transform the spectrum to correct for two problems: (i) change in the signal intensity (or non-linearity) due to scattering and absorbance by the soil surface (Beer's law) and (ii) noise in the signal. Reflectance is converted into absorbance in order to reduce the non-linearity problem:

$$A = \log_{10}(1/R) = -\log_{10} R$$

with A the absorbance and R, the reflectance. Noise reduction is achieved through standard pre-treatments like differentiation and smoothing. Smoothing is used to

diminish random noise around the signal and differentiation to increase the difference between spectral bands. Standard spectral pre-treatments consist of the following:

First and second derivatives. Computing 1st and 2nd derivative may be useful to enhance subtle changes in spectral shape and highlight absorption peaks. Moreover, it allows removing the effects of differences in absolute reflectance induced by variation not related to changes in soil properties (e.g. shadowing).

Gap derivatives. First and second derivatives may increase spectral noise. This problem may be partially overcome by the computation of 1st and 2nd gap derivatives with different window size. The gap derivative implies that the differentiation is not done between two adjacent points x_{i+1} and x_i but between points x_{i-n} and x_{i+n} with 2n+1, the window size.

Savitzky-Golay's smoothing and derivatives. Savitzky-Golay's algorithms are widely used in signal pre-processing (Savitzky and Golay, 1964). They are similar to a moving window averaging method but have the property to better preserve local peaks. The principle is that, for any window [x_{i-n} ; x_{i+n}] centred on a point in position *i* on the spectrum, a polynomial with a given degree is fitted through the points by least square. The fitted value for the point i replaces the measured value. The algorithms involve the use of tabulated coefficient, instead of computing each time the polynomial. An example of Savitzky-Golay algorithms is shown in Figure 8.

Scatter corrections. Difference in particle size between samples may induce different spectral responses due to light scattering. The effects of light scattering are usually minimized by using the Multiplicative Scatter Correction (MSC; Geladi et al., 1985), the Standard Normal Variate transformation and de-trending (SNV and DT; Barnes et al., 1989).

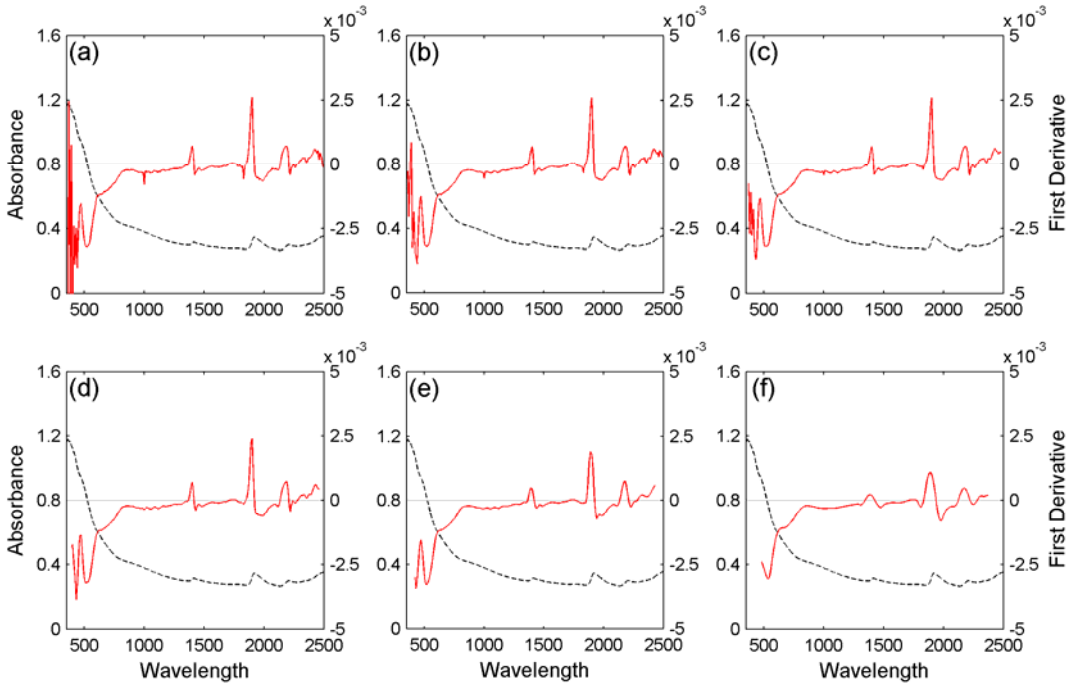

Figure 8. Examples of the effect of different pre-treatments on a laboratory spectrum. Absorbance (black, left scale) is converted to the Savitzky-Golay first derivative (red, right scale) with a window size of (a) 5, (b) 9, (c) 17, (d) 33, (e) 65 and (f) 129 points

3.5.2. Contribution to soil properties mapping

In the case of the hyperspectral approach, the soil property (e.g. Soil Organic Carbon) can be directly related to the spectral information through correlation techniques (usually, chemometrics) using a calibration set. However, there are some constraints in the implementation of such strategy. First, hyperspectral remote sensing is only able to measure the reflectance of the first few millimetres of the surface and can obviously not predict a given property for the entire soil profile. As a consequence, such method of data acquisition may be of little interest when strong vertical gradients in soil properties occur. Secondly, since quantitative prediction of soil properties relies on correlation with spectral data, small changes in spectral features due to environmental changes not directly related to SOC (e.g. soil moisture, roughness, vegetation cover, Fe content, clay content) can have negative impact on prediction accuracy. A conservative approach can be adopted by restricting the prediction to spectra that are similar to the ones used for the calibration (e.g. based on Mahalanobis distance). An independent validation (on a set of samples not covered by the calibration set) must also be carried out to assess the accuracy and reliability of the technique. On the other hand, when some of the other factors affecting the spectral data are known (e.g., surface soil moisture from the GPR data) as well as their effect, such information can be used to unravel SOC estimation and decrease uncertainties in the estimations.

3.6. SEISMIC

Considering seismic methods, we will focus on the exploitation of surface waves by analysing the dispersion behaviour of these waves (SASW), as described in the deliverable D1.1.

3.6.1. Data corrections

Seismic methods, when used for Spectral Analysis of Surface Waves (SASW), do not need any data improvement since the recorded ground motions due to the Rayleigh waves – and used in the SASW – are much more energetic than other kinds of wave, and appear clearly with a good signal to noise ratio in seismograms.

3.6.2. Contribution to soil properties mapping

Near surface methods using elastic wave propagation is conducted at frequencies that vary between a few Hz to a few kHz. In this frequency range, the wavelength in soil ranges between tens of centimetres to tens of meters, therefore the wavelength is much greater then the grain size and the seismic wave propagate without perturbation through the soil mass.

There are three important propagation modes in the near surface: longitudinal propagation (P-wave), transverse propagation (S–wave) and retrograde elliptical Rayleigh wave (R–wave). The shear modulus of the soil G_{soil}, depends on the skeleton shear stiffness, $G_{soil}=G_{sk}$, and is not affected by the bulk stiffness of the pore fluid. For this reason the shear waves are preferred for the characterisation of the near surface deposits. The S–wave velocity Vs is:

$$Vs = \sqrt{\frac{G_{soil}}{\rho_{soil}}}$$

where ρ is the mass density of the soil. The shear modulus is determined by the state of stress, the degree of cementation and by processes that alter inter-particle contacts (capillarity forces, electrical forces). Shear wave velocity can be lower than 20 m/s Figure 9 for soil near suspension to skeleton transition, and can reach 300 m/s to 500 m/s at the depth 30 m. For the unsaturated soils, the bulk stiffness of the fluid is very low, the bulk and shear moduli of the soil mass are those of the soil skeleton. Poisson's ratio is lower than 0.15. For any degree of saturation, the velocity of shear waves is determined by cementation, state of effective stress, capillary forces in silty or clayey soils etc. The propagation of longitudinal P -wave is proportional to constrain modulus M and the masse density ρ

$$Vp = \sqrt{\frac{M_{soil}}{\rho_{soil}}} = \sqrt{\frac{B_{soil} + \frac{4}{3}G_{soil}}{\rho_{soil}}}$$

where B_{soil} is the bulk modulus and G_{soil} is shear modulus of the soil.

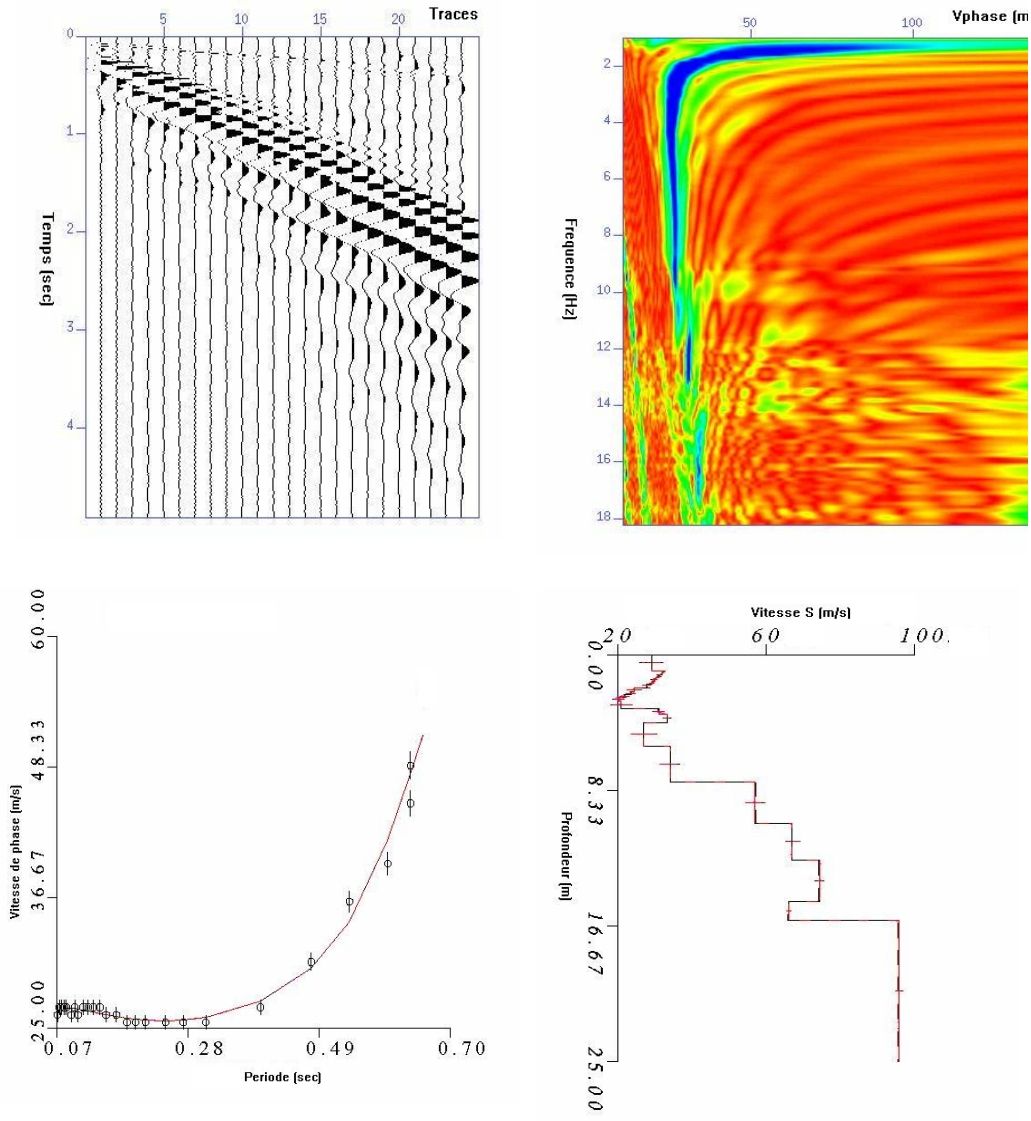

Figure 9 :a-Example of short record with obvious low velocity Rayleigh wave (b)- Phase velocity plot obtained by interception time ray parameter transform c- Experimental and theoretical phase velocity fitting by linear inversion d-Depth variation of shear velocity.

For the saturated soil, the P wave velocity varies between 1500 m/s and about 2000 m/s, depending on porosity. The Poisson's ratio approaches to 0.5. For the unsaturated soil the velocity of the P wave is about 1.4 to 1.6 times higher than shears velocity. The free soil surface promotes the formation of Rayleigh R-wave. The velocity of R –wave V_R is related to the S wave and the P wave velocities and can be estimated as (Santamaria et al. 2005)

$$Vr \approx \frac{0.874 + 1.117\sigma}{1+\sigma} V_S$$

where σ is Poisson's ratio. For unsaturated soils $Vr \approx 0.9V_S$. The R-wave may be used to measure Vs avoiding the need for borehole or probs. The dispersive nature of R-wave propagation in vertically heterogeneous medium forms the basis of surface wave testing (Stokoe et al. 1994, Soco et al. 2004, Matthews et al. 1996,)

For determining bulk density profiles from Vs ones, the use of elastic parameters is mandatory. With the SASW technique, it is useful to obtain a 2D imagery of the density, which can highlight the strong or the weak zone density in an area. Several ways may be performed to obtain the density from the Vs measurements. It is useful to test all of these ways, so as to determine the most accurate method.

1. From empirical relationship between Vs (or Vp) and bulk density

Some empirical relationships can be found between bulk density ρ and shear wave velocity Vs. For saturated soil materials, Burns and Mayne (1996) expressed this relation:

$$\rho = 0.701\,(V_s)^{0.227}\,(\sigma'_{v0})^{-0.057}$$

where σ'_0 is the effective vertical overburden stress in kPa, Vs is in m/s.

Another statistical relationship is presented by Mayne et al. (1999) for gravels, sands, silts and clays:

$$\rho = 1 + \frac{1}{0.614 + 58.7\ (\log z + 1.095)/V_s}$$

where z is the depth in meters, Vs is in m/s.

Some other empirical relations exist between compression wave velocity Vp and either bulk density or porosity. These relations depend on the type of soil, and on the consolidation state. They can be linear or quadratic relations. Then, with using the relation between Vp and Vs with the Poisson coefficient, we obtain a relation between ρ and Vs^2.

2. From the shear modulus G

In this method, we use *in situ* geotechnical parameter q_d, which is the dynamic resistance measured with the PANDA penetrometer.

---

[2] *it is necessary to test these relations and verify if they are adapted to the site. If not, the constant coefficients of these relations could be modified according to the results obtained from the measures.*

Some studies (Gourves and Barjot, 1995) have highlighted correlations between q_d and q_c obtained from the static penetrometer CPT:

$$1\ q_d\ (\text{MPa}) = 1\ \text{CPT}\ (\text{MPa})$$

Then some empirical relations are established between maximum shear modulus G_{max} and q_c, for various types of soils:

For the sand (Lunne et al., 1997):

$$G_{\max} = 1634\ q_c \left(\frac{q_c}{(\sigma'_v)^{1/2}} \right)^{-0.75}$$

σ'_v, q_c et G_{max} in kPa

For the clays (Mayne and Rix, 1993):

$$G_{\max} = 406\ (q_c)^{0.695} e^{-1.130}$$

It must be highlighted that these relations correlate a small strain parameter such as G_{max} with penetration parameter that relates to much larger strains.

Finally with the following elastic relation:

$$G_{\max} = \rho V_s^2$$

We can obtain the bulk density ρ[3].

To check the validity of these correlations and to verify if they are adapted to this context, it could be useful to obtain the bulk density by another measurement.

Thus, some correlations exist between the dynamic resistance q_d measured by the PANDA penetrometer, and the porosity, if the water content is known, as it is demonstrated by Bernard and Dudoignon (2007). Indeed, Perdok et al. (2002) developed with laboratory tests a relation between the resistance according to the porosity and the water content for clays, and sands, and for a water content comprised between 9 to 20 %.

The equation is of the following form:

$$\rho = (1-n)\rho_S + Sr.n.\rho_f$$

[3] *this relation is established in dry soil. It doesn't take into account for the saturation state.*

ρ_s and ρ_f correspond respectively to the solid and fluid densities, *Sr* is the saturation index, *n* is the porosity. For obtaining the *n* value, let assumes that:

$$\log(q_d) = a_0 + a_1 n + w(a_2 + a_3 n)$$

The coefficients a_0, a_1, a_2 and a_3 depend on the nature and the structure of the soil.

To obtain the parameters adapted to the site, if we are in saturated conditions, the equation becomes:

$$\log(q_d) = a_0 + a_1 \frac{\gamma_s w}{1+\gamma_s w} + w(a_2 + a_3 \frac{\gamma_s w}{1+\gamma_s w})$$

So in that case, four values of (w, q_d) are sufficient to establish uniquely this relation[4].

3.7. SOIL MAPS GENERATION

Obtaining soil characteristics maps from geophysical parameters can be a complex topic since relationships between these two sets of quantities are depending on numerous variables. After studying what geophysical parameters bring information on soils characteristics, we propose to design a first flow processing diagram that will be at the basis of future the field testing. Of course this processing methodology will be evaluated and, if necessary, modified after the first acquisition tasks of the project.

[4] *to establish this relation, we need to perform at least 4 measures of q_d and w in a saturated area, where the porosity is supposed to change*

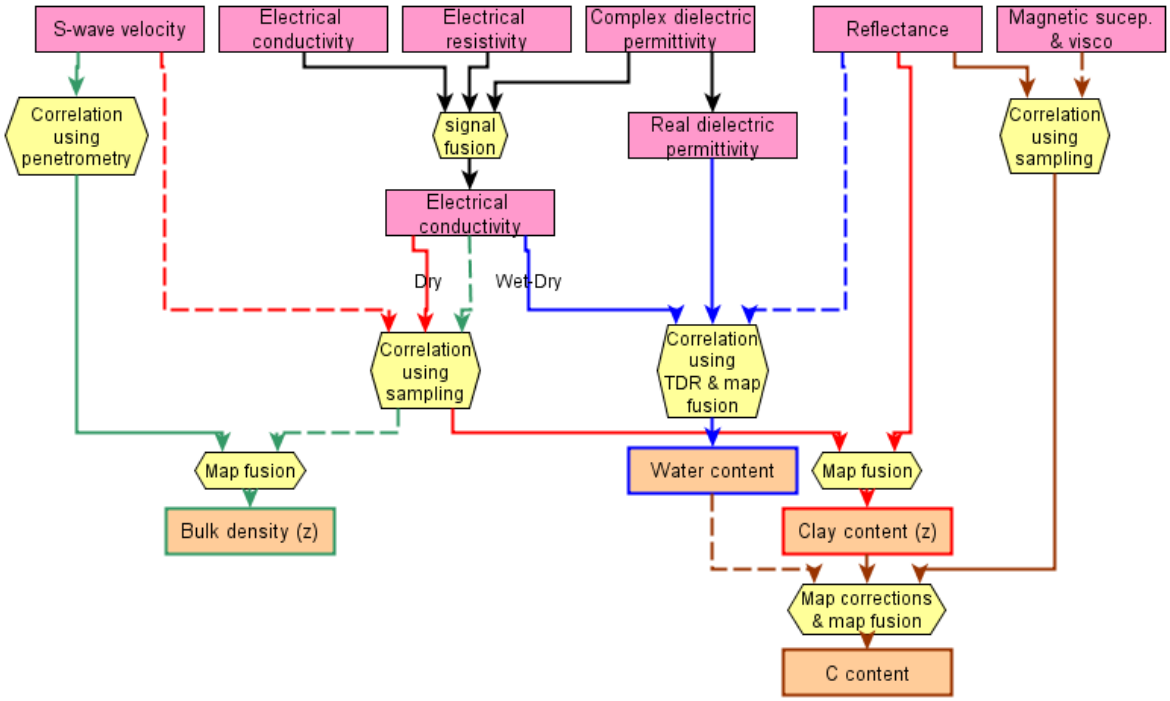

Figure 10 : data assimilation from geophysical parameters to soil properties

According to Figure 10, the estimation of the soil characteristics targeted in the Digisoil project can be based on the following four processes:

3.7.1. Density

- Penetrometry field measurements for calibrating the Vs parameter into density profiles
- Soil sampling and analyses for identifying density profiles and correlation with geoelectric data
- Processing geoelectric, GPR, and seismic data in dry conditions for identifying density profiles and layering structures
- Map fusion between geoelectric, GPR and seismic data

3.7.2. Water content

- Processing reflectance data for extracting high saturated soils at the surface
- Processing GPR/EMI data for mapping soil moisture at the surface and reconstruct vertical water content profiles

- Processing geoelectric data in wet conditions for identifying saturated layers in soils
- TDR Field measurements for calibrating the different source maps
- Map fusion between the reflectance information, the soil moisture map produced from GPR and geoelectric/EMI data;

3.7.3. Clay content

- Processing reflectance data for extracting clayed soils at the surface
- Processing geoelectric/EMI and seismic data in dry conditions for identifying clayed layers in soils
- Soil sampling and analyses for identifying clayed layers and correlation with source data
- Map fusion between the reflectance information, the soil texture map produced from geoelectric, GPR, and seismic data;

3.7.4. C content

- Production of reflectance and magnetic susceptibility maps dedicated to C content mapping
- Soil sampling and analyses for identifying clayed layers and correlation with source data
- C map production using correlations between soil sampling and reflectance and magnetic susceptibility maps
- Correction of C map using clay and water content maps

3.8. VALIDATION STRATEGY

Validation will be essentially based on soil sampling and laboratory analyses, at least at the beginning of the project for estimating the performances of the proposed methodologies. For example, considering magnetism, the first step of the validation strategy is to map magnetic properties over areas with contrasted organic matter content. It will validate the conditions under which the magnetic properties are relevant as a proxy to spatialize the organic matter content. It will lead to the definition of an operational protocol for the measurements on the test fields.

4. Conclusions

The present deliverable concerns the first task of the DIGISOIL's WP2. During this study, we started to analyze the requirements for making soil characteristics maps and the way to use and integrate geophysical parameters for this purpose. After a state of the art on the different solutions for assimilating different sources for improving the quality of such maps, we proposed a review of the capabilities of each method for characterizing soil structures and properties.

A general processing workflow was then established. It constitutes a first technical solution to reach our objectives. It will be tested in the future by using data acquired during the next field acquisition missions. This processing takes into account the different geophysical sensors already identified, supposes that inversion algorithms have already been applied to that data, uses auxiliary data for corrections, calibration or validation.

At the end of the task WP2.1, we finalized the part of the system dealing with the generation of the soil properties maps, as shown on the *Figure 11*.

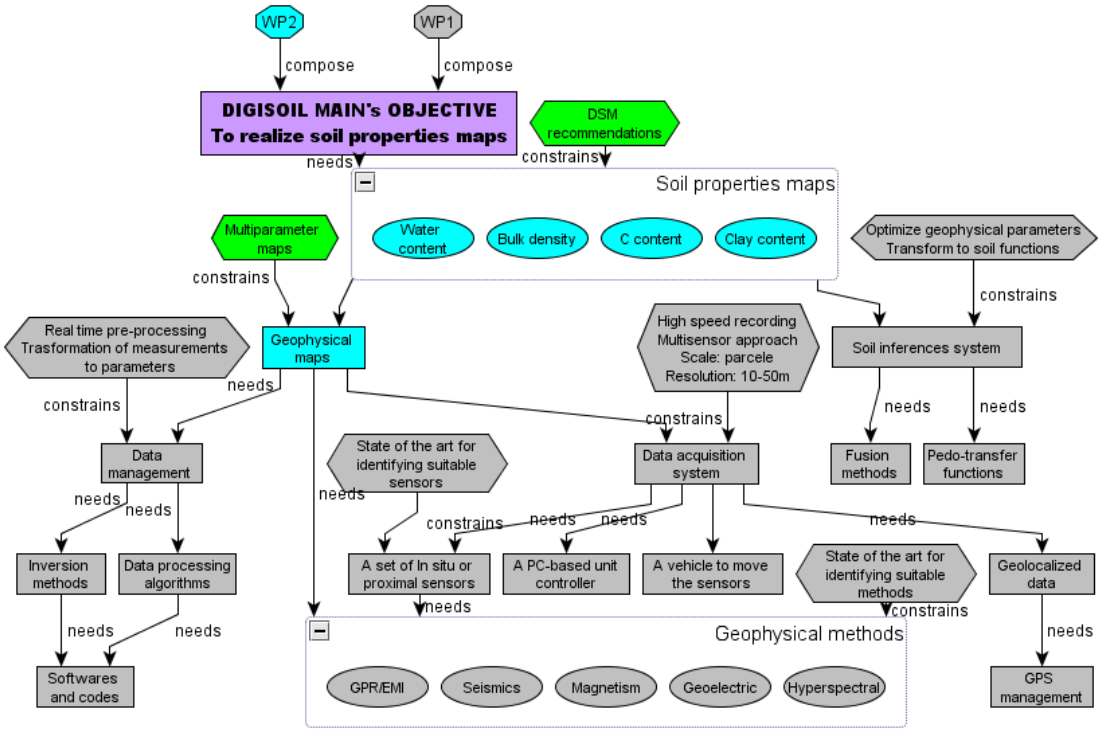

Figure 11 : Schematic functional analysis of the Digisoil production: deliverable D2.1 tasks are highlighted

5. References

Archie, G.E. 1942. The electrical resistivity log as an aid in determining some reservoir characteristics. Trans. Am. Inst. Min. Metall. Pet. Eng. 146:54-62.

Barnes, RJ, MS Dhaona and SJ Lister. 1989. Standard Normal Variate transformation and detrending of near-infrared diffuse reflectance spectra. *Applied Spectroscopy,* 43: 772-777.

Bayes, T., 1763. An Essay towards solving a Problem in the Doctrine of Chances, Philosophical Transactions of the Royal Society of London, 53:370-418.

Bernard M., Dudoignon P., 2007. Corrélation profils de résistance à la pointe – profiles de teneur en eau dans les sols argileux : Marais de Rochefort. 25èmes rencontres de l'AUGC, 23-25 mai 2007, Bordeaux.

Besson, A., I. Cousin, A. Dorigny, M. Dabas, and D. King. 2008. The temperature correction for the electrical resistivity measurements in undisturbed soil samples: Analysis of the existing conversion models and proposition of a new model. Soil Sci. 173 (10): 707-720.

Besson A., Cousin I., Bourennane H., Nicoullaud B., Pasquier C., Richard G., King D., 2009. The spatial and temporal organisation of the soil water content at field scale as described by electrical resistivity measurements. European Journal of Soil Science (accepted)

Besson, A., I. Cousin, A. Samouëlian, H. Boizard, and G. Richard. 2004. Structural heterogeneity of the soil tilled layer as characterized by 2D electrical resistivity surveying. Soil and Tillage Research 79:239-249.

Burns, S.E., Mayne, P. W. 1996. Small- and high-strain measurements of in-situ soil properties using the seismic cone penetrometers. TRR 1548 Small-Magnitude Measurements in Geotechnical Engineering. National Academy Press, pp. 81-88.

Campbell, R.B., C.A. Bower, and L.A. Richards. 1948. Change of electrical conductivity with temperature and the relation of osmotic pressure to electrical conductivity and ion concentration for soils extracts. Soil Sci. Soc. Am. Proc. 13:66-69.

Cierniewski, J. and Courault, D. 1993. Bidirectional reflectance of bare soil surfaces in the visible and near-infrared range. Remote Sensing Reviews 7, 321-339.

Corwin, D.L., and S.M. Lesch. 2005. Apparent soil electrical conductivity measurements in agriculture. Computers and Electronics in Agriculture 46:11-43.

Dobson, M.C., F.F. Ulaby, M.T. Hallikainen, and M.A. El-Rayes. 1985. Microwave dielectric behavior of wet soil - Part II: Dielectric mixing models. IEEE Transactions on Geoscience and Remote Sensing 23:35-46.

Feingersh, T., Ben-Dor, E. Filin, S. 2009. Correction of reflectance anisotropy: a multi-sensor approach. International Journal of Remote Sensing, *submitted*.

Fukue, M., T. Minato, H. Horibe, and N. Taya. 1999. The micro-structure of clay given by resistivity measurements. Engineering Geology. 54:43-53.

Geladi, P, D MacDougall and H Martens. 1985. Linearization and scatter-correction for near-infrared reflectance spectra of meat. *Applied Spectroscopy,* 39: 491-500.

Grandjean, G., Malet, J.P., Bitri, A., and Meric O., 2007. Geophysical data fusion by fuzzy logic for imaging mechanical behaviour of mudslides. Bull. Soc. Geol. France, 177, 2, 133-143.

Gourves R. and Barjot R., 1995. The PANDA ultralight dynamic penetrometer for soil investigation. Proc 11th Euro. Conf. on Soil Mechanics and Foundation Engineering, 28th May – 1st June 1995 Copenhagen.

Hamilton, E.L., 1970. Sound velocity and related properties of marine sediments. North Pacific. J. Geophys. Res., 75., 4423-4446.

Hendrickx, J.M.H., B. Das, D.L. Corwin, J.M. Wraith, and R.G. Kachanoski. 2002. Relationship between soil water solute concentration and apparent soil electrical conductivity, p.1275-1282, In J.H. Dane and J.C. Topp, eds. Methods of Soils Analysis: part 4. Physical methods. Soil Science Society of America, Madison, WI, USA.

Hermann, R.B., 1987. Computer programs in seismology. Saint-Luis University, USA.

Hilhorst, M.A. 1998. Dielectric characterization of soil, Wageningen Agricultural University, Wageningen, The Netherlands.

Huisman, J.A., C. Sperl, W. Bouten, and J.M. Verstraten. 2001. Soil water content measurements at different scales: accuracy of time domain reflectometry and ground penetrating radar. Journal of Hydrology 245:48-58.

Jadoon, K.Z., E. Slob, M. Vanclooster, H. Vereecken, and S. Lambot. 2008. Uniqueness and stability analysis of hydrogeophysical inversion for time-lapse ground penetrating radar estimates of shallow soil hydraulic properties. Water Resources Research W09421, doi:10.1029/2007WR006639.

Kalinski, R.J., and W.E. Kelly. 1993. Estimating water content of soils from electrical resistivity. Geotechnical Testing Journal 16:323-329.

Kalman, R.E., 1960. A New Approach to Linear Filtering and Prediction Problems, Transactions of the ASME - Journal of Basic Engineering, Vol. 82: pp. 35-45.

Kowalsky, M.B., S. Finsterle, J. Peterson, S. Hubbard, Y. Rubin, E. Majer, A. Ward, and G. Gee. 2005. Estimation of field-scale soil hydraulic and dielectric parameters through joint inversion of GPR and hydrological data. Water Resources Research 41:W11425, doi:10.1029/2005WR004237.

Lambot, S., E.C. Slob, I. van den Bosch, B. Stockbroeckx, and M. Vanclooster. 2004. Modeling of ground-penetrating radar for accurate characterization of subsurface electric properties. IEEE Transactions on Geoscience and Remote Sensing 42:2555-2568.

Lambot, S., I. van den Bosch, B. Stockbroeckx, P. Druyts, M. Vanclooster, and E.C. Slob. 2005. Frequency dependence of the soil electromagnetic properties derived from ground-

penetrating radar signal inversion. Subsurface Sensing Technologies and Applications 6:73-87.

Ledieu, J., P. De Ridder, P. De Clercq, and S. Dautrebande. 1986. A method of measuring soil moisture by time domain reflectometry. Journal of Hydrology 88:319-328.

Lesch, S.M., and D.L. Corwin. 2003. Using the dual-pathway parallel conductance model to determine how different soil properties influence conductivity survey data. Agronomy Journal 95:365-379.

Lunne P., Robertson P. K., Powell J. J. M., 1997. Cone penetration testing in geotechnical practice. E and FN SPON.

M. T. v. G. a. F. J. L. a. L. Wu (ed.) 1994. Proc. Time Domain Reflectometry, Applications in Soil Science, Research Centre Foulum, Denmark. SP-Report 25-33, Danish Inst. of Plant and Soil Sci., Tjele, Denmark.

Matthews, M.C., Hope, V.S., Clayton, R.I.,1996. The use of surface waves in the determination of ground stifness profiles. Proc. Instn. Geotech. Engng., 119, 84-95.

Mayne, P. W., Schneider, J.A., and Martin, G. K., 1999. Small- and large-strain soils properties from seismic flat dilatometer tests. Proceeding, Pre-failure deformation characteristics of geomaterials, Torino ’99, Balkema, Rotterdam, 8 pp.

Mayne, P. W., and Rix, G., J., 1993. Gmax – qc relationship for clays. Geotechnical Testing Journal, ASTM, Vol. 16, No. 1, pp. 54-60.

McCarter, 1984 W.J. McCarter, The electrical resistivity characteristics of compacted clays, Géotechnique 34 (1984), pp. 263–267.

Michot et al., 2003 D. Michot, Y. Benderitter, A. Dorigny, B. Nicoullaud, D. King and A. Tabbagh, Spatial and temporal monitoring of soil water content with an irrigated corn crop cover using electrical resistivity tomography, Water Resour. Res. 39 (2003), p. 1138.

Mokhtar, T. A., Herrmann, R. B., and Russel, D. R. 1988 Seismic velocity and Q model for the shallow structure of the Arabian shield from shot-period Rayleigh waves, Geophysics, 53, 1379-1387

Perdok U. D., Kroesbergen B. and Hoogmoed W. B., 2002. Possibilities for modelling the effect of compression on mechanical and physical properties of various Dutch soil types. Soil and Tillage Research, 65:61-75.

Rhoades, J.D., P.A.C. Raats, and R.J. Prather. 1976. Effects of liquid-phase electrical conductivity, water content, and surface conductivity on bulk soil electrical conductivity. Soil Science Society of America Journal 40:651-655.

Rhoades, J.D., N.A. Manteghi, P.J. Shouse, and W.J. Alves. 1989. Soil electrical conductivity and soil salinity: new formulations and calibrations. Soil Science Society of America Journal 53:433-439.

Robinson, D.A., I. Lebron, S.M. Lesch, and P. Shouse. 2004. Minimizing drift in electrical conductivity measurements in high temperature environments using the EM-38. Soil Science Society of America Journal 68:339-345.

Robinson, D.A., S.B. Jones, J.M. Wraith, D. Or, and S.P. Friedman. 2003. A review of advances in dielectric and electrical conductivity measurement in soils using time domain reflectometry. Vadose Zone Journal 2:444-475.

Santamarina J.C, Rinaldi V.A., Fratta D., Klein K.A., Wang Y.H., Cho G..C., Cascante G. A. 2005. Survey of Elastic and electromagnetic properties of near surface soils. In Near Surface Geophysics. Investigation in geophysics No 13.

Savitzky, A and MJE Golay. 1964. Smoothing and differentiation of data by simplified least squares procedures. *Analytical Chemistry,* 36: 1627-1638.

Sheets, K.R., and J.M.H. Hendrickx. 1995. Noninvasive soil-water content measurement using electromagnetic induction. Water Resources Research 31:2401-2409.

Schon, J.H., 1996., Physical properties of rocks; Fundamentals and principles of petrophysics., Seismic Exploration, Vol 18, 583p.

Socco, L.V and Strobbia, C., 2004. Surface-wave method for near-surface characterization: a tutorial. Near Surface Geophysics, 165-185.

Stokoe, K.H, Wright, G.W., James, A.B., and Jose, M.R., 1994, Characterisation of geotechnical sites by SASW method, in Geophysical characterisation of site, ISSMFE Technical Committee # 10 edited by R.D Woods, Oxford Publishers, New Delhi

Thomas, E.C., 1992. 50th anniversary of the Archie's equation, Log Analysts, May-June, 199-205.

Topp, G., J.L. Davis, and A.P. Annan. 1980. Electromagnetic Determination of Soil Water Content: Measurements in Coaxial Transmission Lines. Water Resources Research 16:574-582.

Weiler, K.W., T.S. Steenhuis, J. Boll, and K.J.S. Kung. 1998. Comparison of ground penetrating radar and time domain reflectometry as soil water sensors. Soil Science Society of America Journal 62:1237-1239.

West, L.J., K. Handley, Y. Huang, and M. Pokar. 2003. Radar frequency dielectric dispersion in sandstone: Implications for determination of moisture and clay content. Water Resources Research 39(2):1026, doi:10.1029/2001WR000923.

Wraith, J.M., and D. Or. 1999. Temperature effects on soil bulk dielectric permittivity measured by time domain reflectometry: experimental evidence and hypothesis development. Water Resources Research 35:361-369.

Scientific and Technical Centre
ARN Division
3, avenue Claude-Guillemin - BP 36009
45060 Orléans Cedex 2 – France – Tel.: +33 (0)2 38 64 34 34